Roles of inter-SWCNT junctions in resistive humidity response

Zhang, Kang; Zou, Jianping; Zhang, Qing

2015

Zhang, K., Zou, J., & Zhang, Q. (2015). Roles of inter-SWCNT junctions in resistive humidity response. Nanotechnology, 26, 45501-.

https://hdl.handle.net/10356/83002

https://doi.org/10.1088/0957-4484/26/45/455501

Roles of Inter-SWCNT Junctions in Resistive Humidity Response

Kang Zhang, Jianping Zou and *Qing Zhang**

Dr. K. Zhang, Dr. J. Zou, Prof. Q. Zhang

Centre for Micro-/Nano-electronics (NOVITAS)
School of Electrical & Electronic Engineering
Nanyang Technological University
639798 Singapore, Singapore
E-mail: eqzhang@ntu.edu.sg

Abstract

As a promising chemiresistor for gas sensing, single-walled carbon nanotube (SWCNT) network has not been fully utilized for humidity detection. In this work, it is found that, as humidity increases from 10% to 85%, the resistance of as-grown SWCNT networks first decreases and then increases. Such non-monotonic resistive response to humidity limits their sensing capabilities. The competition between SWCNT resistance and inter-tube junction resistance changes is then found responsible for the non-monotonic resistive humidity responses. Moreover, creating sp^3 scattering centers on SWCNT sidewall by monovalent functionalization of 4-bromobenzene diazonium tetrafluoroborate (4-BBDT) is shown to be capable of eliminating the influence from the inter-tube junctions, resulting in a continuous resistance drop as humidity increases from 10% to 85%. Our results revealed the competing resistive humidity sensing process in as-grown SWCNT networks, which could also be helpful in designing and optimizing as-grown SWCNT networks for humidity sensor and other gas sensors.

Keywords: carrier hopping, covalent functionalization, sensitivity

1. Introduction

SWCNT random networks have been extensively studied for gas sensing due to their high specific surface area, high chemical stability and excellent mechanical properties. [1,2] In many studies, SWCNT sensors prepared by simply depositing a pair of metal electrodes onto a random SWCNT network could be much more sensitive to testing gases than the traditional solid-state resistive gas sensors. [3-5] It is noted that recent advances in solid-state gas sensors have revealed that nanostructured metal oxides and 2D material based gas sensors could provide comparable or even higher sensitivity than SWCNT sensors for many testing gases. [23-25] However, SWCNT network still has its own advantages over the above mentioned nanomaterials for sensing applications due to its high stability in ambient air and high tunability by many available functionalization techniques. In spite of the simple structures of many SWCNT network sensor devices, the sensing mechanisms of SWCNT networks response to various gases are rather complex. The responses may originate from modulation of the SWCNT resistance, variation of the metal/SWCNT contact resistance and change in the inter-tube junction resistance between two adjacent SWCNTs. [6-8]

Humidity sensor is a type of gas sensor that has a broad variety of applications in meteorology, electronic applications, automobiles, medical services, industry, agriculture, biotechnology, and manufacturing, etc. [9,10] However, there has been little research on SWCNT network based resistive humidity sensors. Although drop-casted SWCNT films have been used for resistive humidity sensing, [4,5] their responses were shown to originate from the carrier hopping at the junctions between the SWCNTs and/or the SWCNT bundles rather than from the SWCNT sidewalls. As a result, these devices could not fully utilize the large surface to volume ratio of

SWCNTs and, moreover, their sensitivities and selectivities are difficult to be tailored through sidewall modifications to the SWCNTs. In contrast, as-grown SWCNT networks typically consist of much longer individual nanotubes with less inter-tube junctions (as compared to drop-caseted SWCNT film) and, thus, they are potentially a better chemresistor for humidity sensing applications. However, the existence of both metallic and semiconducting SWCNTs, and the junctions between them could result in complex responses to humidity changes. In this work, as-grown SWCNT networks with various nanotube densities are investigated on their resistive humidity responses. The roles of the SWCNTs and the inter-tube junctions are identified, and in addition, covalent functionalizations are shown to significantly increase the sensitivity and the detection dynamic range of the as-grown SWCNT network humidity sensors. Our results reveal the competing resistive humidity sensing process in as-grown SWCNT networks, and demonstrate the capability of as-grown SWCNT network for humidity sensing applications. This work could also be helpful in designing and optimizing as-grown SWCNT networks for other gas sensors.

2. Results and Discussion

2.1 Characterization of As-grown SWCNT Random Networks

SWCNT networks are grown on quartz substrate in a thermal-CVD reactor at 925 ℃ using ferritin as the catalyst precursor. [11] The morphologies of as-grown SWCNTs are first characterized by scanning electron microscopy. Figure 1b and 1c show the as-grown SWCNT network with low density and high density of SWCNTs, respectively. The density of SWCNT network is estimated by counting the number of SWCNTs per unit area in AFM images. The densities of the as-grown SWCNT networks used in this work are between ~ 1 μm^{-2} and ~ 13 μm^{-2}. SWCNT networks with the nanotube

density less than ~1 μm^{-2} were generally found to have higher electrical noise probably due to the poor percolation of SWCNTs.

The properties of the as-grown SWCNTs networks are then characterized using Raman spectroscopy as well as atomic force microscopy (AFM). Similar to our previous results, [11] a mixture of metallic and semiconducting SWCNTs with a diameter distribution of ~1.0 – 2.2 nm is confirmed by Raman scattering with the incident laser wavelength of 532 nm and 633 nm (Figure 2b and 2c). AFM measurement shown in Figure 2a further confirms the diameter distribution of the as-grown SWCNTs.

The electrical conductance of as-grown SWCNT networks is also characterized and their conductance versus density curves is consistent with standard percolation theory with appropriate fitting parameters. [12] The total conductance of an as-grown SWCNT random network could be modeled by the expression $\sigma = k(N - N_C)^{\alpha}$, [12] where σ is the total conductance of the network, k is a proportional constant, N is the volume loading of the nanotubes in mg/L, N_C is the critical volume loading of nanotubes (mg/L) corresponding to the percolation threshold, and α is the fitting exponent. The critical volume loading is determined by the length scale of the nanotubes with the expression $N_C = 1/\pi(4.236/L)^2$ mg/L, [12] where L is the average length of the nanotubes in μm. By assigning the proportional constant $k = 1.7 \times 10^{-7}$, the critical fitting exponent $\alpha = 1.94$, [12, 13] the effective nanotube length $L = 50\ \mu m$, and the conversion ratio of mass per unit volume (mg/L) over nanotube loading per unit area (μm^{-2}) equals 1, the average conductances measured for the as-grown networks are in good agreement with the standard percolation theory (see Figure 3). The standard deviations of the resistances are within

0.5% (see Figure 3 inset) by sampling the resistance every 1 sec with a constant dc voltage of 1 V applied to the electrodes for 2 min.

2.2 Humidity Response of SWCNT Networks – Identify the Role of Inter-tube Junctions

As illustrated in Figure 1a, humidity devices are fabricated by depositing a pair of Ti/Au at both ends of the SWCNT networks. The contacts between the nanotubes and the electrodes were covered by 300 nm thick silicon nitride to prevent humidity from affecting the contact resistance between the electrodes and nanotubes. The resistive humidity test was conducted in a test chamber, whose humidity levels were varied by controlling the relative flow ratio between dry air and humid air. The normalized resistances of four SWCNT networks with different densities are plotted versus their humidity levels. As shown in Figure 4a, when humidity increased from 10% to 85%, the total resistance of the SWCNT networks first decreased and then increased. Therefore, for each curve of the resistance versus humidity, there existed a 'critical humidity' (as labeled in Figure 4a) beyond which the SWCNT network resistance started to increase. The 'critical humidity' levels for twelve SWCNT networks are plotted versus their densities in Figure 4b. It can be seen that the "critical humidity" was between 30% and 45 % for SWCNT networks with nanotube loading larger than 6.8 μm^{-2}. For SWCNT networks with nanotube loading less than 6.8 μm^{-2}, the 'critical humidity' levels became higher. The influence of SWCNT network density on the 'critical humidity' level is explained in supporting information. In this work, we use "monotonic" response to describe the case where the SWCNT random network resistance continuously increases or decreases as humidity increases from 10% to 85%. In contrast, a "non-monotonic" response refers to the case where the resistance does not change in one direction as humidity increases from 10% to 85%.

Due to the non-monotonic resistance versus humidity, as-grown SWCNT networks were therefore not suitable for humidity sensing applications.

In order to understand the non-monotonic resistive humidity responses of above SWCNT networks, it is important for us to study the roles of the nanotubes themselves and their junctions. Since a random SWCNT network consists of SWCNTs with a large variety of chiralities, it is difficult to identify the role of a particular SWCNT. However, it is possible for us to determine the collective humidity response of SWCNTs in a horizontally aligned array in which roles of inter-tube junctions should not be considered. As shown in Figure 5a, the humidity sensing device was fabricated on a quartz substrate with horizontally aligned SWCNT array and no inter-tube junction could be observed under SEM. The resistance of the SWCNTs parallel to the conduction channel decreased monotonically as humidity increased from 10% to 85% and no 'critical humidity' was observed, which is in sharp contrast to SWCNT random networks. As the horizontally aligned SWCNTs grew under the same conditions as those random SWCNT networks, they had very similar SWCNT chirality distributions as confirmed by Raman scatterings. Thus, the only difference in the humidity responses must originate from the inter-tube junctions. As a result, the increase of SWCNT network resistance beyond the 'critical humidity' must be caused by the inter-tube junctions.

To further verify the hypothesis, two horizontally aligned SWCNT array devices with low and high degree of crosslinking SWCNTs were also compared with their humidity responses. As shown in Figure 5b and 5c, the 'critical humidity' appeared on both devices due to the crosslinking. In addition, the high crosslinking area circled in Figure 5c showed a much larger resistance increase and a much lower 'critical humidity'. Therefore, we could suggest that, as humidity increase, the overall resistive

response of an as-grown SWCNT network is actually a competition between two mechanisms, i.e. the resistance drop caused by all the SWCNTs and the resistance increase due to all the inter-tube junctions. The ‘critical humidity’ thus represents the relative humidity at which the two mechanisms are balanced.

The finding that inter-tube junction resistance increases with increasing humidity is consistent with previous theoretical predictions in drop-casted SWCNT films, where the origin was explained through the suppression of inter-tube carrier hopping by water molecules. [5] As humidity increases, the average separation between SWCNTs at the tube-tube contact will also be increased so that the thermally activated carrier hopping at inter-tube junctions is suppressed, resulting in an increase in the inter-tube resistance. [5] However, the resistive humidity response of horizontally aligned SWCNTs array without inter-tube junctions has been little studied. It is well understood that the resistance decrease of an SWCNT could be achieved by either increasing carrier densities or reducing carrier scatterings. Carrier concentration could be increased through electron doping from water molecules to semiconducting SWCNTs. [14-17] However, the doping mechanism is not sufficient to explain the monotonic drop of SWCNT array resistance over the entire humidity range. This is because the electrons transferred from water molecules to semiconducting SWCNTs would first decrease hole concentration and then increase electron concentration due to the inherent p-type nature of semiconducting SWCNTs in air. [4] Therefore, in order to explain the monotonic drop of SWCNT resistance, there must be other mechanism(s) in which the carrier scattering in SWCNTs could be reduced by water molecules. Actually, there has been studies [18-21] suggesting that the response of SWCNT to chemical vapors is mainly contributed through the defect sites that are typically low energy adsorption centers, and the trapped molecules could contribute to

the electrical conductance *via* the Poole-Frenkel (PF) conduction. Thus, in the presentce of defects, water molecules could easily attach to the SWCNTs and decrease the resistances of both metallic and semiconducting SWCNTs *via* the Poole-Frenkel (PF) conduction.

2.3 Effects of Covalent Functionalization on Humidity Sensing Responses of SWCNT Networks

In order to use as-grown SWCNTs random networks as a humidity sensor element, the influences from the inter-tube junctions must be eliminated. For this purpose, the SWCNTs are modified through covalent functionalization which has two apparent effects on the sensing behaviors of the SWCNT networks. On one hand, it could create additional defects on SWCNTs and increase their resistance by a few orders of magnitude so that the total resistance is largely limited by the SWCNTs rather than the inter-tube junctions. Thus, the resistance changes of the SWCNTs by adsorbing water molecules dominate the overall resistive response of the SWCNT network so that the detection range of the humidity sensor could be largely extended. On the other hand, the created defects could enhance hydrophilicity of the SWCNTs and, at the same time, increase the influences *via* the Poole-Frenkel (PF) conduction mechanism. [18-21]

An SWCNT random network with nanotube density of ~ 6.8 μm^{-2} was subjected to low-degree and high-degree covalent functionalizations by soaking the sample into a 10 μM 4-bromobenzene diazonium tetrafluoroborate (4-BBDT) solution at room temperature for 1 min and 5 min, respectively. [22] The device was subsequently washed thoroughly in deionized water and annealed at 120 ℃ in air for 2 min to fully remove the chemical residual. The SWCNTs were successfully functionalized as manifested by the Raman D band (~1340 cm^{-1}) to G band (~1580 cm^{-1}) ratio (I_D/I_G)

increase as shown in Figure 6c and 6e. (The Raman spectra are calculated by averaging all the 100x100 points in a Raman mapping on a 10 μm × 10 μm square). Figure 6c shows a higher I_D/I_G than Figure 6b, indicating that higher concentration defects are created under a longer reaction time.

As seen in Figures 6b, 6d and 6f, the 'critical humidity' level shifted from 30% to 45% after 1 min functionalization and further shifted to 75% after 5 min functionalization. This finding suggests that at a higher defects concentration, the humidity response originating from the SWCNTs dominates over the humidity response from the inter-tube junctions due to the significant increase in SWCNT resistance. As shown in Figure 2, the resistance is increased by more than two orders after 5 min of the functionalization. Therefore, the total resistance of the SWCNT network is now significantly limited by the functionalized SWCNTs, and the change in the SWCNT resistance should also have a much larger effect to the overall resistance. As a result, SWCNT resistance become a stronger dominant over the inter-tube junctions and thus shifts the 'critical humidity' towards a higher value. In addition, the addend groups also significantly increase the hydrophilicity of the SWCNTs, resulting in a huge increase of sensitivity from less than 5% to more than 25%. The shift of "critical humidity" and increase in sensitivity by 4-BBDT functionalization is also observed in SWCNT networks with lower and higher densities as shown in supporting information Figure S3.

The sensor response of the SWCNT network at different defect concentrations are also compared with a relative humidity between 10% and 30%, and between 45% and 75% at time intervals of 30 seconds. As seen in Figure 7a, the sensitivity of the SWCNT network subject to 10% and 30% humidity is much increased by the functionalization. In Figure 7b, it is shown that the pristine network had its resistance

slightly increased when the relative humidity was increased from 45% to 75%. In contrast, after the functionalization, the SWCNT network had its resistance decreased when the relative humidity is increased from 45% to 75%. In addition, the sensitivity of the SWCNT network was also increased by the functionalization due to the increased hydrophilicity of the SWCNTs by attaching covalent molecules.

It has been noticed that significant drifts of response curve baseline was observed in both Figure 7a and Figure 7b. In Figure 7a, there is a down-drift of the resistance as humidity switches between 10% and 30%. Referring to Figure 6, the resistance of the pristine, 1 min and 5 min functionalized samples tends to decrease when humidity is increased from 10% to 30%. However, the resistance values shown in Figure 6 are taken at stabilized states, and it requires about 20 min for the resistance value to be stabilized after humidity is switched from 10% to 30%. In contrast, the humidity switching in Figure 7a is carried out in 30 sec short intervals, so that the unsaturated adsorption (when humidity switched from 10% to 30% humidity) and incomplete desorption (when humidity switched from 30 back to 10%) of water molecules to and from the SWCNTs are responsible for the down-drift.

In Figure 7b, the humidity is switched between 45% and 75%, and there is an up-drift for the pristine and 1 min functionalized samples, but a down-drift of the 5 min functionalized sample. Referring to the response curves in Figure 6b and 6d, for the pristine and 1 min functionalized samples, when humidity is switched from 45% to 75%, their total resistance will increase due to the inter-tube junctions. Therefore, the up-drift of the pristine and 1 min functionalized samples in Figure 7b is due to the unsaturated adsorption and incomplete desorption of water molecules at the inter-tube junctions in the 30 sec short intervals. In contrast, as shown in Figure 6f, for the 5 min functionalized sample, when humidity is switched from 45% to 75%, the total

resistance decreases due to the SWCNT resistance drop. Therefore, the down-drift of the 5 min functionalized sample in Figure 7b is due to the unsaturated adsorption and incomplete desorption of water molecules to the SWCNTs in the 30 sec short intervals.

It is worth noting the response curve of the 1 min functionalized sample in Figure 7b. The overall trend of the total resistance is an up-drift when humidity is changed from 45% to 75% at 30 sec intervals. This overall up-drift trend is consistent with the stabilized resistance curve in Figure 6b where increasing humidity from 45% causes an increase in resistance. However, the transient resistive response at the switching is opposite to the up-drift trend, i.e. at the moment when humidity is switched from 45% to 75%, there is always a resistance drop rather than increase. Therefore, there must be different mechanisms governing the up-drift trend and the transient resistance decrease when humidity switched from 45% to 75%. As discussed earlier, the resistance decrease of the SWCNT networks is caused by the SWCNTs, while the resistance increase is caused by the inter-tube junctions. Therefore, this abnormal response curve in Figure 7b further suggests that the overall resistive humidity response of the SWCNT networks is a competition between the SWCNT resistance change and inter-tube junction resistance change. In addition, the opposite transient response also implies that the response from the SWCNTs could be much faster than the responses from the inter-tube junctions.

3. Conclusion

In this work, the non-monotonic resistance versus humidity relationship of SWCNT networks is first investigated. Through humidity response comparisons among sensor devices with SWCNTs parallel to the conduction channel at different crosslinking levels, it is suggested that the overall resistive humidity response of a SWCNT

network is actually the competition between SWCNTs and inter-tube junctions. The mechanism that SWCNTs in response to humidity is largely contributed by the Poole-Frenkel conduction through the defects on the SWCNT sidewalls. In contrast, inter-tube junctions play a crucial role in limiting the SWCNT network conductance through the suppression of inter-tube carrier hopping by water molecules. [5] Covalent modifications to the SWCNTs are shown capable to enhance the humidity detection dynamic ranges by increasing the resistance of the SWCNTs, and increase the sensitivities of as-grown SWCNT networks to humidity by increasing its hydrophilicity. Moreover, the observation of opposite transient response to the overall resistance drift suggests that the response from the SWCNTs should be faster than the response originates from the inter-tube junctions.

Experimental

SWCNT Network Device Fabrication: Thermal CVD growth of SWCNT networks on quartz substrate was conducted in a quartz tube furnace at 925 °C with ferritin as catalyst precursor and ethanol as carbon source. [16] The densities of the SWCNT networks are controlled by varying the catalyst densities. Humidity sensors were fabricated by depositing pairs of Ti/Au electrodes onto the SWCNT networks on quartz substrates (~ 1 cm × 1 cm) through shadow masks. In order to exclude possible influences of the contacts between the electrodes and SWCNT network on sensing responses, A 300 nm thick silicon nitride passivation layer was deposited onto the contact areas, leaving only the SWCNT network exposed to the environment.

Humidity Response Measurement: Resistive humidity responses of the SWCNT networks were measured in a sensor chamber where the relative humidity could be changed by changing the relative flow ratio of dry air and humidly air (through a

deionized water bubbler). The total flow rate is set to 1000 sccm so that the entire volume of the chamber (~ 300 cm^3) could be effectively filled by the test gases in less than 1 min. The resistance of the SWCNT network device was sampled every 1 sec with a constant 1 V dc voltage applied. The SWCNT network resistance values at different humidity levels are recorded after the resistance is stabilized at each humidity levels.

Raman Spectroscopy: Raman spectroscopy was used to determine the diameter distribution of the pristine SWCNTs as well as to determine the degree of defects in the functionalized SWCNTs. Raman scattering was performed with excitation laser lines of 532 nm and 633 nm using a confocal Raman system in air and calibrated with the silicon peak ~ 520 cm^{-1}. Raman mappings of SWCNT networks were performed on random 10 um $\times$ 10 um squares with 100 $\times$ 100 points resolution.

Acknowledgements

The authors would like to thank their colleagues at Centre for Micro-/Nano-electronics (NOVITAS), School of Electrical & Electronic Engineering, Nanyang Technological University for valuable discussions. "The project is financially supported by MOE AcRF Tier2 Funding, Singapore (MOE2013-T2-2-100) and MOE AcRF Tier1 Funding, Singapore (2014-T1-001-268, RG 105/14)."

Received: ((will be filled in by the editorial staff))

Revised: ((will be filled in by the editorial staff))

Published online: ((will be filled in by the editorial staff))

References:

[1] Kauffman D R and Star A 2008 *Angew. Chem. Int. Ed.* **47** 6550

[2] Zhang T, Mubeen S, Myung N V and Deshusses M A 2008 *Nanotechnology* **19** 332001

[3] Salehi-Khojin A, Khalili-Araghi F, Kuroda M A, Lin K Y, Leburton J P and Masel R I 2011 *ACS Nano* **5** 153

[4] Han J W, Kim B, Li J and Meyyappan M 2012 *J. Phys. Chem. C* **116** 22094

[5] Ling Y F, Gu G R, Liu R Y, Lu X J, Kayastha V, Jones C S, Shih W S and Janzen D C 2013 *J. Appl. Phys.* **113** 024312

[6] Bradley K, Gabriel J C P, Star A and Gruner G 2003 *Appl. Phys. Lett.* **83** 3821

[7] Liu X L, Luo Z C, Han S, Tang T, Zhang D H and Zhou C W 2005 *Appl. Phys. Lett.* **86** 243501

[8] Peng N, Zhang Q, Chow C L, Tan O K and Marzari N 2009 *Nano Lett.* **9** 1626

[9] Story P R, Galipeau D W and Mileham R D 1995 *Sensor. Actuat. B-Chem.* **25** 681

[10] Dessler A E and Sherwood S C 2009 *Science* **323** 1020

[11] Zou J P, Zhang K, Li J Q, Zhao Y B, Wang Y L, Pillai S K R, Demir H V, Sun X W, Chan-Park M B and Zhang Q 2015 *Sci. Rep.* **5** 11755

[12] Stauffer D, Aharony A 1994 *Introduction to percolation theory*, Taylor & Francis London, Bristol PA

[13] Li J T and Zhang S L 2010 *Phys. Rev. E* **81** 021120

[14] Rinkio M, Zavodchikova M Y, Torma P and Johansson A 2008 *Phys. Status. Solidi. B* **245** 2315

[15] Sung D, Hong S, Kim Y H, Park N, Kim S, Maeng S L and Kim K C 2006 *Appl. Phys. Lett.* **89** 243110

[16] Kim W, Javey A, Vermesh O, Wang O, Li Y M and Dai H J 2003 *Nano Lett.* **3** 193

[17] Pati R, Zhang Y, Nayak S K and Ajayan P M 2002 *Appl. Phys. Lett.* **81** 2638

[18] Jombert A S, Coleman K S, Wood D, Petty M C and Zeze D A 2008 *J. Appl. Phys.* **104** 094503

[19] Salehi-Khojin A, Field C R, Yeom J and Masel R I 2010 *Appl. Phys. Lett.* **96** 163110

[20] Robinson J A, Snow E S, Badescu S C, Reinecke T L and Perkins F K 2006 *Nano Lett.* **6** 1747

[21] Watts P C P, Mureau N, Tang Z N, Miyajima Y, Carey J D and Silva S R P 2007 *Nanotechnology* **18** 175701

[22] Wang C J, Cao Q, Ozel T, Gaur A, Rogers J A and Shim M 2005 *J. Am. Chem. Soc.* **127** 11460

[23] Late D J, Huang Y K, Liu B, Acharya J, Shirodkar S N, Luo J J, Yan A M, Charles D, Waghmare U V, Dravid V P and Rao C N R 2013 *ACS Nano* **7** 4879

[24] Miller D R, Akbar S A and Morris P A 2015 *Sensor. Actuat. B-Chem.* **211** 569

[25] Perkins F K, Friedman A L, Cobas E, Campbell P M, Jernigan G G and Jonker B T 2013 *Nano Lett.* **13** 668

Figures

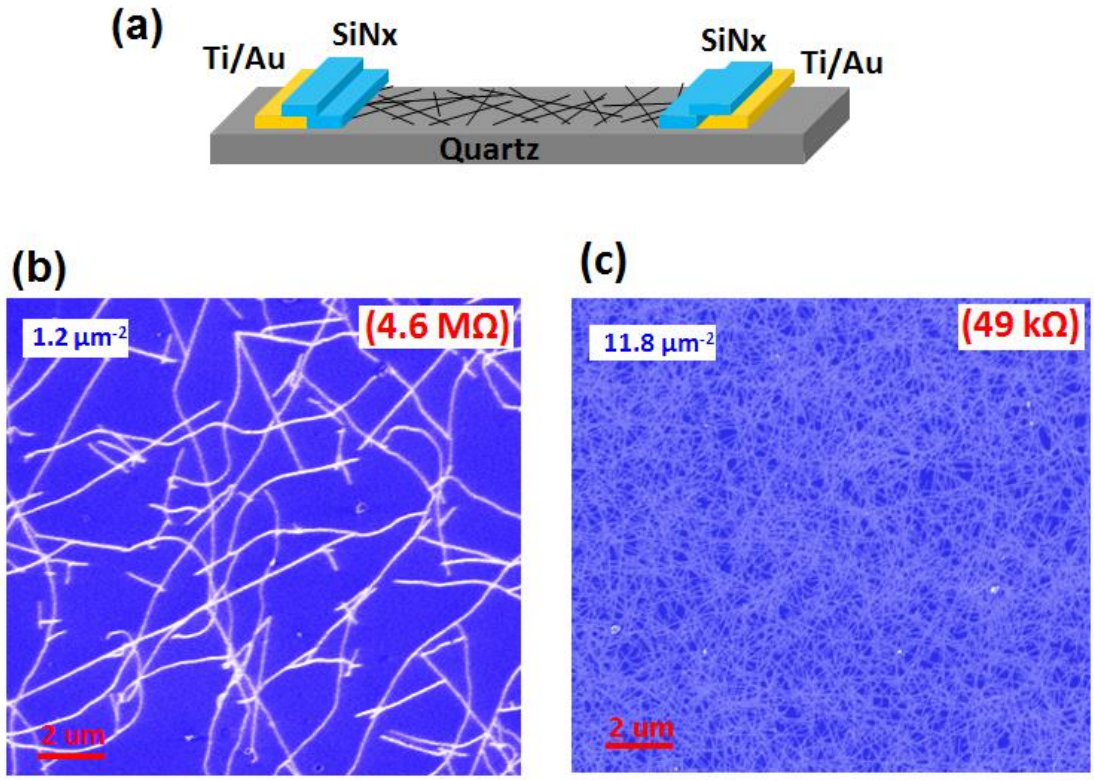

Figure 1

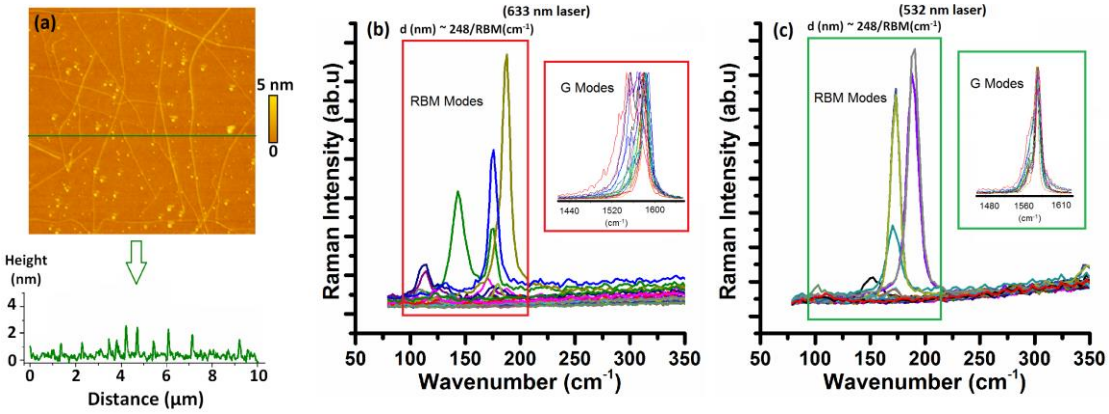

Figure 2

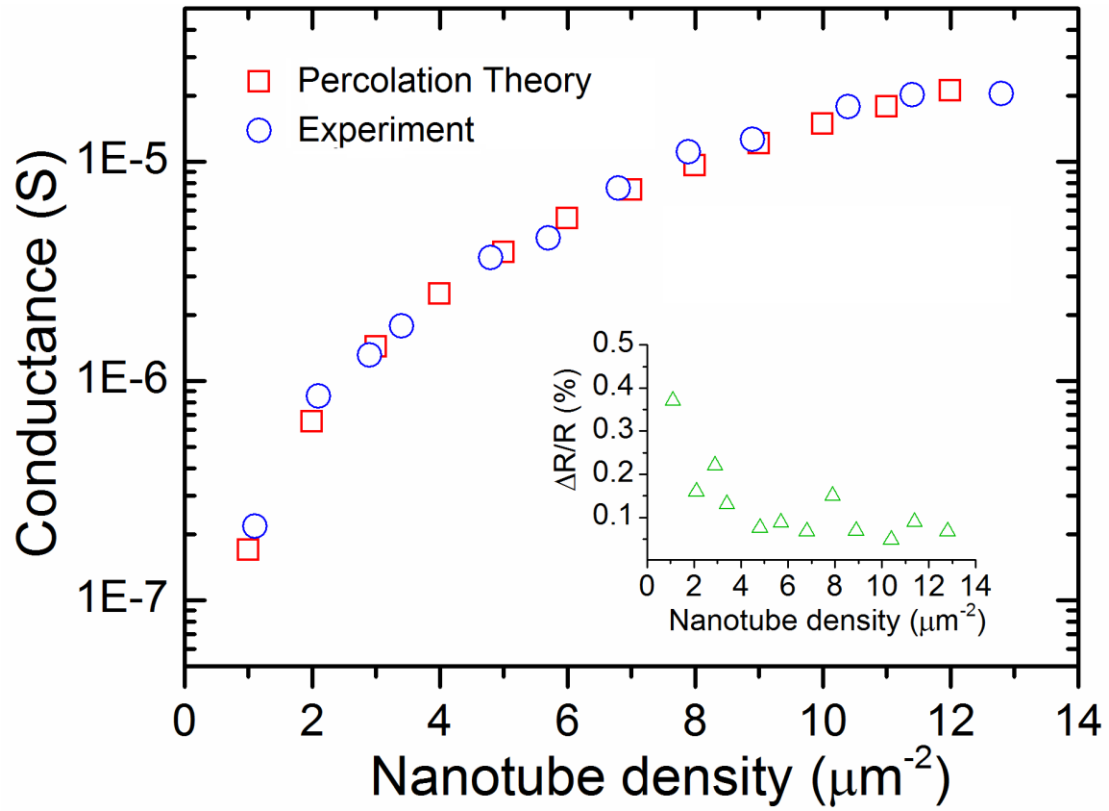

Figure 3

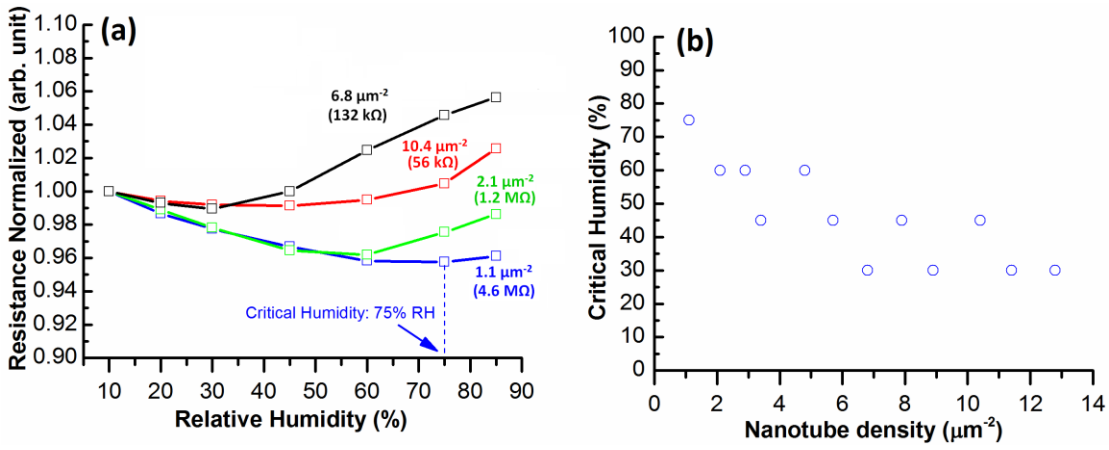

Figure 4

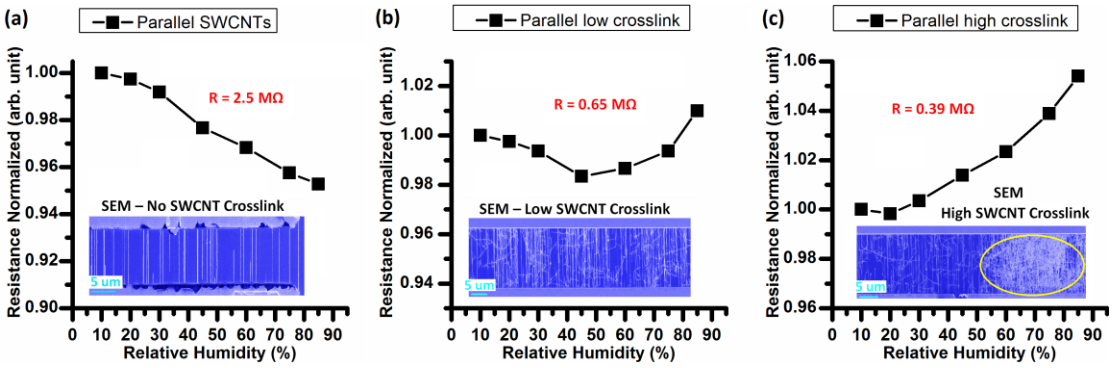

Figure 5

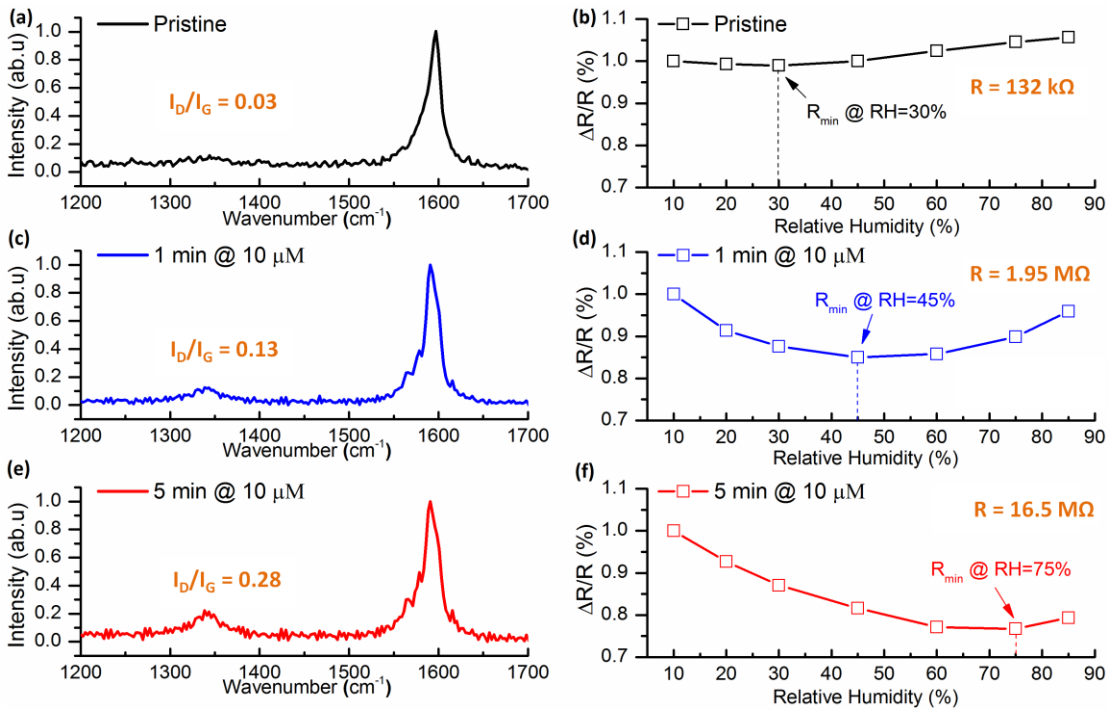

Figure 6

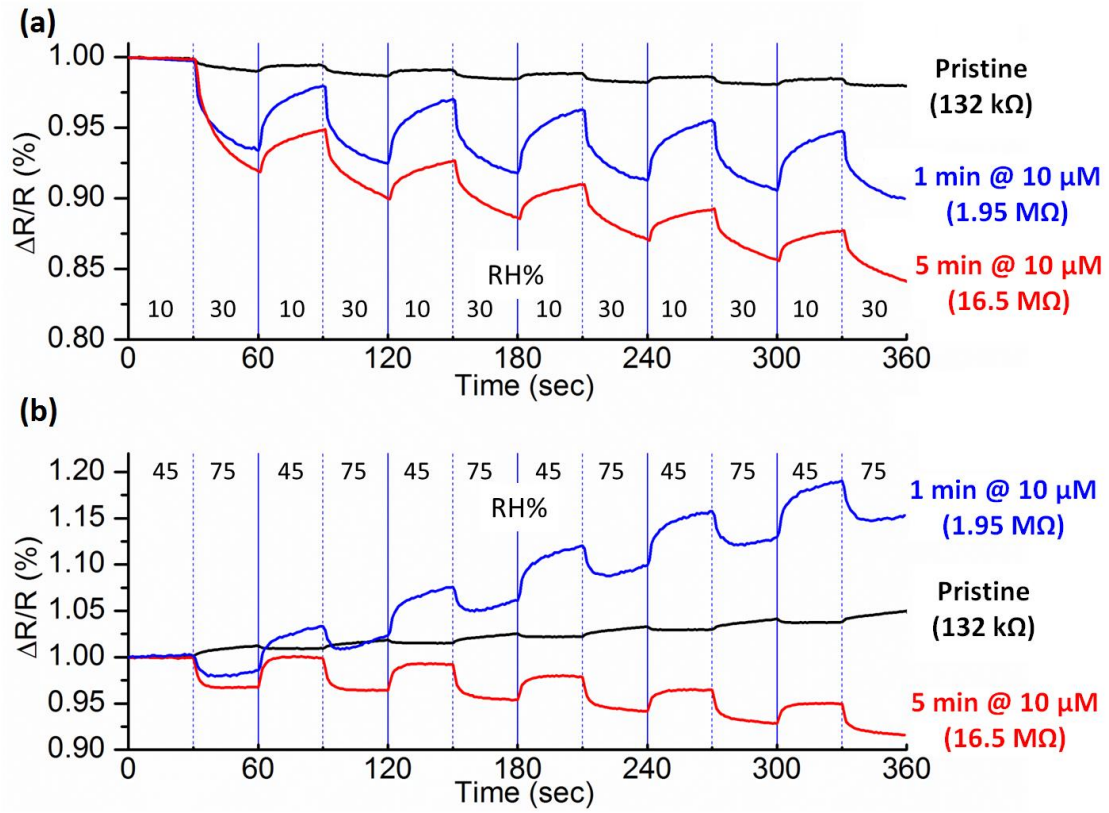

Figure 7

Figure Captions:

Figure 1. Schematic of an SWCNT network humidity sensor. (a) Schematic of the devices structure. (b) SEM image of as-grown low density SWCNT network. (c) SEM image of as-grown high density SWCNT network.

Figure 2. Characterization of as-grown SWCNTs by AFM and Raman scattering. (a) AFM height measurement of as-grown SWCNTs. (b) The Raman scattering radial breathing modes and G modes of SWCNTs under 633 nm laser excitation. (c) The Raman scattering radial breathing modes and G modes of SWCNTs under 532 nm laser excitation.

Figure 3. SWCNT network conductance versus the nanotube density. The experimental data (circle) is fitted to calculated results (square). Inset shows the

standard variation of the SWCNT network resistances sampled every 1 second with a constant dc voltage of 1.0 V.

Figure 4. The percentage resistance change of the SWCNT networks at different relative humidity levels. (a) Resistance change of four SWCNT networks with nanotube density of 1.1 μm^{-2}, 2.1 μm^{-2}, 6.8 μm^{-2} and 10.4 μm^{-2}, respectively. Inset: The SEM images of the SWCNT networks. (b) The 'critical' humidity of the SWCNT network sensors versus the SWCNT densities.

Figure 5. Humidity response of horizontally aligned SWCNT arrays with (a) no inter-tube junctions, (b) a low degree of crosslinking and (c) a high degree of crosslinking, respectively. Inset: The SEM images of the SWCNT arrays.

Figure 6. The effect of covalent functionalization (4-BBDT reaction) on the humidity response of the as-grown SWCNT network with nanotube density of ~ 6.8 μm^{-2}. (a) The Raman scattering of the pristine SWCNT network. (b) The percentage resistance change of the pristine SWCNT network at different relative humidities. (c) The Raman scattering of the SWCNT network after 1 min 4-BBDT reaction. (d) The percentage resistance change of the SWCNT network after 1 min 4-BBDT reaction. (e) The Raman scattering of the SWCNT network after 5 min 4-BBDT reaction. (f) The percentage resistance change of the SWCNT network after 5 min 4-BBDT reaction.

Figure 7. Comparison of the humidity response of the SWCNT network with nanotube density of ~ 6.8 μm^{-2} at different defects levels. (a) The percentage

resistance change of the SWCNT network, at pristine state, after 1 min 4-BBDT functionalization and after 5 min 4-BBDT functionalization, respectively, subject to relative humidity switching between 10% and 30% at 30 s intervals. (b) The percentage resistance change of the SWCNT network, at pristine state, after 1 min 4-BBDT functionalization and after 5 min 4-BBDT functionalization, respectively, subject to relative humidity switching between 45% and 75% at 30 s intervals.

Supporting Information

Roles of Inter-SWCNT Junctions in Resistive Humidity Response

Kang Zhang, *Jianping Zou* and *Qing Zhang**

Dr. K. Zhang, Dr. J. Zou, Prof. Q. Zhang
Centre for Micro-/Nano-electronics (NOVITAS)
School of Electrical & Electronic Engineering
Nanyang Technological University
639798 Singapore, Singapore

E-mail: eqzhang@ntu.edu.sg

1. Resistive Humidity Responses Influenced by the Density of As-grown SWCNT Networks

According to the data obtained in Figure 4b, the "critical humidity" level is higher than 45% for SWCNT random network with density less than 6.8 μm^{-2}. While for the SWCNT random networks having densities larger than 6.8 μm^{-2}, the "critical humidity" is always around 30% to 45% with no clear trend. As the "critical humidity" level is determined by the competition between SWCNT resistance and inter-tube resistance change, SWCNT random networks with density less than 6.8 μm^{-2} have larger dependence on SWCNTs. While for SWCNT random networks with density above 6.8 μm^{-2}, the dependence on SWCNTs is dropped and the competition between SWCNTs and inter-tube junctions become stabilized. Figure S1 is drawn to assist the explanation to the observation.

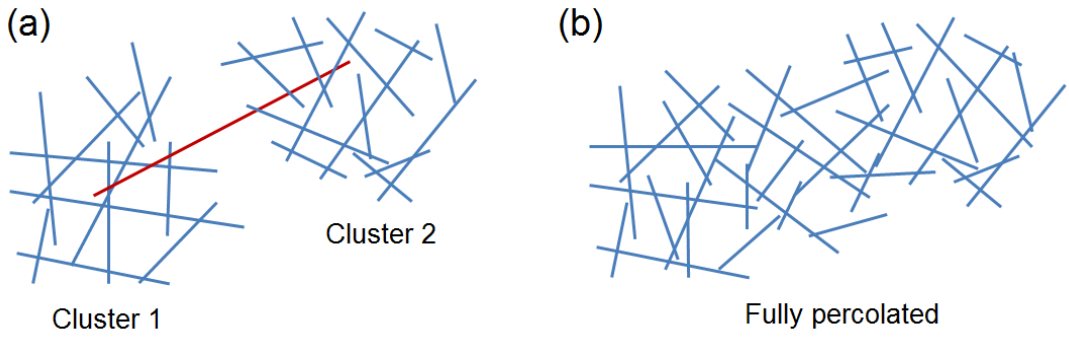

Figure S1 Stick illustration of the SWCNT percolating connections in (a) a low and (b) a high density SWCNT random network.

As shown in Figure S1a, in a low density random network, the percolation of SWCNTs is still not effective, and there are regions where two percolated clusters are connected by only one long SWCNT (marked RED in Figure S1a). In that case, the resistance of the SWCNT network is dominated by some individual SWCNTs, rather than the contact resistance between these SWCNTs and the clusters. Upon humidity

change, the resistance change of particular individual SWCNTs would represent the overall resistance variation of the random network.

As shown in Figure S1b, once SWCNTs in a random network are fully percolated, the extra available conduction paths reduce the conduction dependence on the particular individual SWCNTs.

2. Effect of Covalent Functionalization on the Resistive Humidity Responses of SWCNT Networks

The humidity responses of as-grown SWCNT networks at different densities are compared before and after the 4-BBDT functionalization. The covalent functionalization by 4-BBDT is expected to significantly degrade the conductance of the SWCNTs, resulting a much larger R_{CNT}/R_{Junct} ratio. Figure S2 shows the resistance drop of four SWCNT networks with different densities. As seen in Figure S2, the conductances of the SWCNT networks are dropped by about two orders after 5 min of 4-BBDT functionalization.

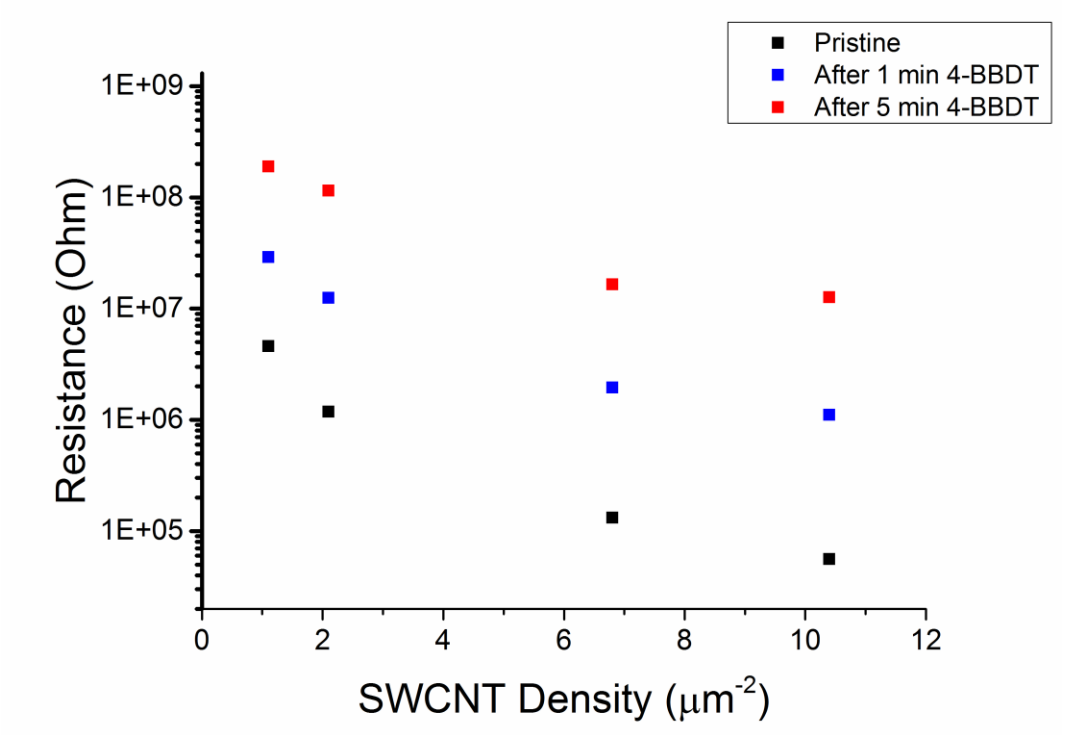

Figure S2 Comparison of resistance of SWCNT networks, with densities of 1.1 μm^{-2}, 2.1 μm^{-2}, 6.8 μm^{-2} and 10.4 μm^{-2}, before and after 4-BBDT functionalization.

Due to the significant drop of SWCNT resistance, the humidity responses from the inter-tube junctions (i.e. resistance increase by water molecules) has much smaller contributions to the overall response of the SWCNT network, which is expected to shift the "critical humidity" levels to a higher value. In addition, the defects sites created by the functionalization serve as trapping centers for water molecules, making the SWCNTs much more hydrophilic and sensitive to environmental humidity changes.

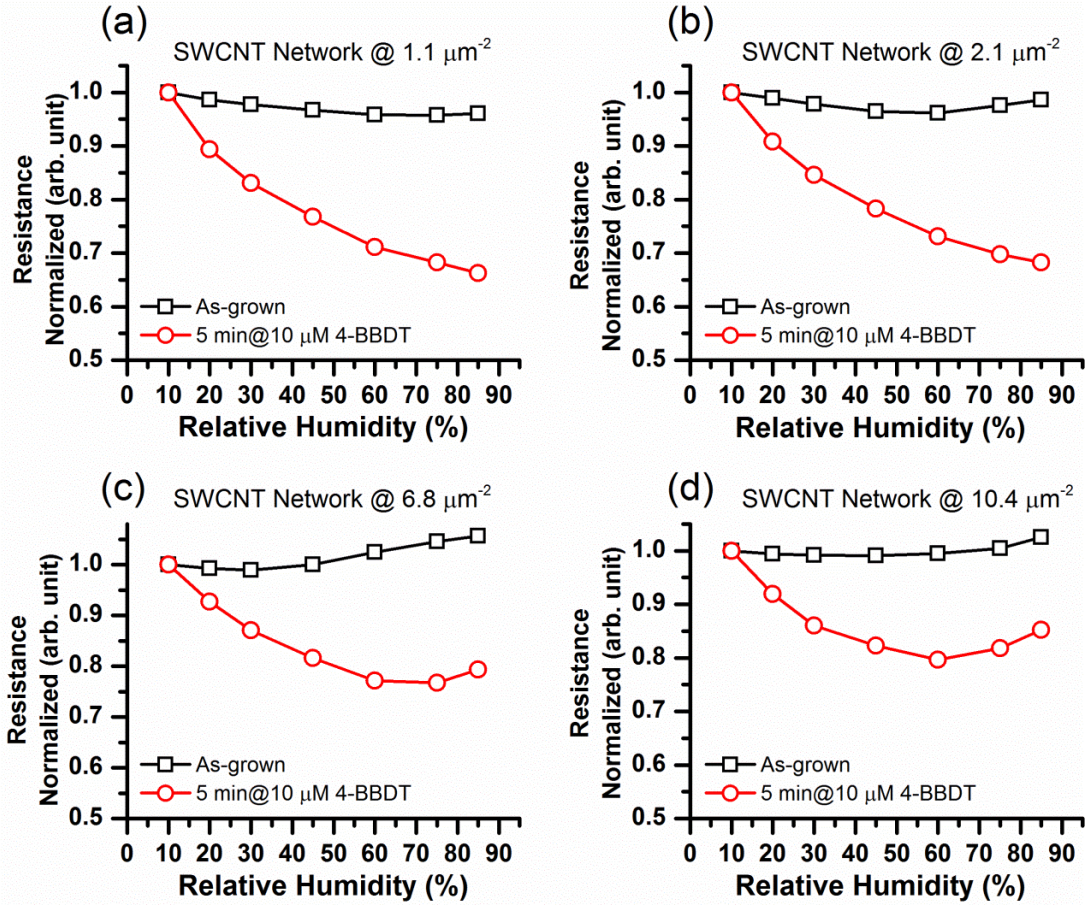

Figure S3 Humidity responses of the SWCNT networks with a density of 1.1 μm^{-2} (a), 2.1 μm^{-2} (b), 6.8 μm^{-2} (c), 10.4 μm^{-2} (d) before and after 5 min of covalent functionalizations by 4-BBDT.

As shown in Figure S3, all SWCNT networks have stronger resistive response after their respective functionalization, suggesting a much high sensitivity towards humidity changes. In addition, the humidity ranges for the resistance drop is extended for all the SWCNT networks. Especially for SWCNT networks with density of 1.1 μm^{-2} (Figure S3a) and 2.1 μm^{-2} (Figure S3b), their resistance drop monotonically over the whole humidity range from 10% to 85% after the functionalization.